Geomorphology 102 (2008) 567–577

Contents lists available at ScienceDirect

Geomorphology

journal homepage: www.elsevier.com/locate/geomorph

Terrain maps displaying hill-shading with curvature

Patrick J. Kennelly *

Department of Earth & Environmental Science, C.W. Post Campus of Long Island University, 720 Northern Blvd., Brookville, NY 11548, USA

ARTICLE INFO

Article history:
Received 8 January 2008
Received in revised form 30 May 2008
Accepted 31 May 2008
Available online 8 June 2008

Keywords:
Planimetric curvature
Profile curvature
Illumination
Shaded relief
Cartography
Geographic visualization

ABSTRACT

Many types of maps can be created by neighborhood operations on a continuous surface such as provided by a digital elevation model. These most commonly include first derivatives slope or aspect, and second derivatives planimetric or profile curvature. Such variables are often used in geomorphic analyses of terrain. First derivatives also provide subtle enhancements to hill-shaded maps. For example, some maps combine oblique and vertical illumination, with the latter reflecting variations in slope.

This study illustrates how second derivative maps, in conjunction with hill-shading, can cartographically enhance topographic detail. A simple conic model indicates that image-tone edges where slope or aspect varies by less than 0.5° are visible on curvature maps. Hill-shaded images combined with curvature enhance the continuity of naturally occurring tonal edges, especially in strongly illuminated areas. Variations in planimetric and profile curvature seem to be especially effective at highlighting convergent and divergent drainages and variations in erosion rate between or within sedimentary units, respectively. Shading curvature with consideration given to illumination models can add detail to hill-shaded terrain maps in a manner similar to cognitive models employed by map viewers.

1. Introduction

Geomorphologists and cartographers both employ variables derived from elevation data to quantify the shape or structure of topographic surfaces (Robinson et al., 1995; Wilson and Gallant, 2000; Slocum et al., 2004; Li et al., 2004). This study focuses on the cartographic representation of variables computed from local (neighborhood) operations directly from the topographic data, the "primary attributes" discussed in Wilson and Gallant (2000). Also addressed are operations that treat the terrain as a continuous function $f(x,y,z)$ and compute first and second order derivatives.

First order derivatives include slope gradient and slope aspect. Slope, the rate of change in elevation (the z-value), quantifies the steepness of terrain. Aspect is the compass direction of steepest slope. Second order derivatives include profile and planimetric curvature, which are measured along and across the direction of maximum slope, respectively (Evans, 1972; El-Sheimy et al., 2005; Chang, 2006).

Geomorphology focuses on the patterns of these attributes and why they are significant to Earth surface processes (Table 1, column 2). Contour lines (Table 1, column 3) represent the intersection of topography with a series of planes parallel to a datum separated by a constant z-interval, while tonal contrasts and elevation derivatives, the focus of cartographic research, help visualize the terrain (Table 1, column 4).

Contours can be used to estimate slope, aspect, and curvature alone. Elevation can be read directly from contour labels, and the spacing or the change in spacing among contours indicates changes in slope and profile curvature, respectively. An orthogonal vector defined by two nearby contours on a map yields aspect, and the curve of the contour itself shows the change in aspect or planimetric curvature.

Contours, however, can require added information if the viewer is to translate them into a cognitive model of a topographic surface. For example, are two concentric, closed contours a depression or a hilltop? Determination would require reading contour values, looking for hachures, or viewing the contours in the context of the overall terrain. Also, having *a priori* knowledge of an area's geomorphology may be helpful (e.g. karst vs. fluvially carved terrain). One visual aid frequently applied in discriminating high vs. low is layer or hypsometric tinting (Imhof, 1965; Robinson et al., 1995), in which background colors change with elevation. Color schemes are designed to be intuitive, reflecting common variations associated with changes in elevation. For example, tints may progress from green to brown to white with increasing elevation in mountainous areas.

Contours create image tones that mimic maps with vertical illumination (Imhof, 1965). Viewers have a difficult time distinguishing shapes under such lighting. The Tobacco Root mountains of Montana are shown in Fig. 1 with contours (a) and "slope shading" from vertical illumination (b). Although some hand- and computer-contouring techniques overcome this visualization problem (e.g. Tanaka, 1932, 1950; Peucker et al., 1975; Yoeli, 1983; Kennelly and Kimerling, 2001; Kennelly, 2002), such techniques are not widespread.

* Tel.: +1 516 299 2652; fax: +1 516 299 3945.
E-mail address: Patrick.Kennelly@liu.edu.

0169-555X/$ – see front matter © 2008 Elsevier B.V. All rights reserved.
doi:10.1016/j.geomorph.2008.05.046

Table 1
Basic attributes of topography, their geomorphic significance, and their cartographic representation

Attribute	Geomorphic/geographic significance		Cartographic representation
Elevation	Climate, vegetation, potential energy	CONTOURS	Layer tinting
Slope	Flow velocity & runoff, vegetation, soil-water content, capability class		Slope shading
Aspect	Solar insolation, evapotranspiration, flora and fauna distribution/abundance		HILL SHADING Aspect color schemes with azimuthal luminance variations
Planimetric curvature	Converging/diverging flow, soil-water content, soil characteristics		Grayscale or divergent color scheme
Profile curvature	Flow acceleration rate, erosion/ depostion rate		Grayscale or divergent color scheme

Excerpted and elaborated from Table 1.1, p. 7 of Wilson and Gallant (2000).

Map users find that oblique illumination, a light source shining from a moderate angle between the horizon and zenith, and from the northwest, provides more intuitive images of the shape of the terrain (Imhof, 1965; Horn, 1981; Robinson et al., 1995; McCullagh, 1998; Slocum et al., 2004). Imhof (1965) cites westerners' preference for general room lighting when writing and drawing (from above and the left) as the reason for this psychological effect. Many map viewers see inversion of terrain when illuminated from the opposite direction. Properly illuminated, such hill-shaded or shaded relief maps are popular for their realistic look and detail (e.g. Thelin and Pike, 1991). Hill-shading is calculated as:

$$BV = 255\cos\theta \tag{1}$$

where BV is the 8-bit (0 to 255) grayscale brightness of each hill-shaded surface element (0 is black and 255 is white), and θ is the angle between a constant illumination vector and a normal vector to the terrain at each given locale. As such, hill-shading is a function of both slope and aspect, and its formula can also be written as:

$$BV = 255\cos I\sin S\cos(A-D) + \sin I\cos S \tag{2}$$

where I and D are the inclination from horizontal and azimuthal declination of the illumination vector, and S and A are the slope and aspect values.

Although hill-shaded maps are rich in visual information, and useful for solving specific geomorphological problems (Oguchi et al., 2003; Smith and Clark, 2005; Van Den Eeckhaut et al., 2005), default computer applications may limit cartographic freedom to enhance particular features of importance (Thelin and Pike, 1991; Allan, 1992; Patterson, 2004). Some cartographers such as those with the Swiss Institute of Cartography, elevated manual hill-shading to an art form, including

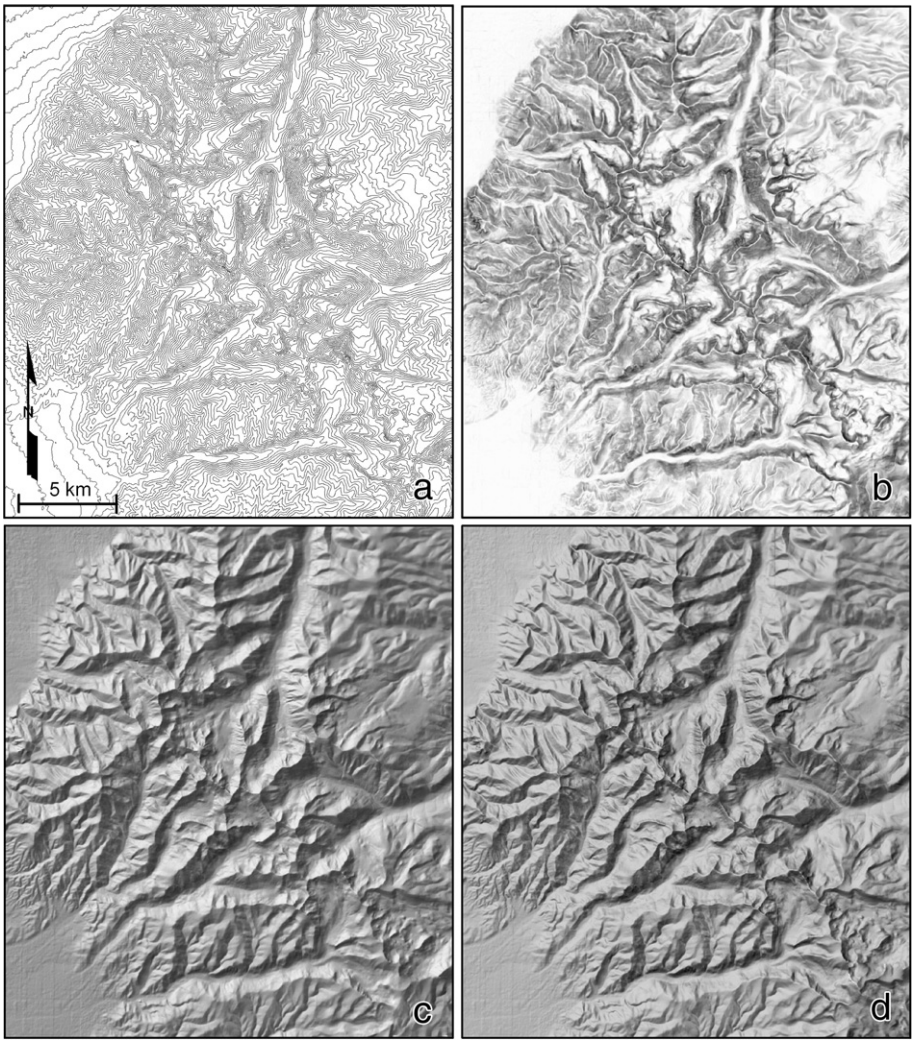

Fig. 1. Four maps of the Tobacco Root mountains of southwestern Montana: a) unlabeled contours, b) slope shading following "the steeper the darker", c) conventional hill-shading with oblique northwestern illumination, and d) combined hill-shading from the northwest and vertical illumination.

combining hill-shading with slope shading to highlight steep terrain (Imhof, 1965). Computer-assisted cartographers combine the two in a similar manner to provide additional information about the shape of the terrain in a visually harmonious manner (Patterson and Herman, 2004). I include in Fig. 1 examples of the Tobacco Root Mountains with hill-shading (c), and hill-shading combined with slope shading (d). The latter adds some visual emphasis to ridge lines and valleys, especially those oriented parallel to the direction of illumination (i.e. northwest to southeast).

Representing aspect on a map is a challenge because aspect is a cyclical variable; north has a value of both 0° and 360°. Cartographic researchers have addressed this problem by devising new aspect color schemes, where luminosity or lightness of colors approximates or complements tonal variations associated with hill-shading. Moellering and Kimerling (1990) chose easily discriminated colors, and varied them with aspect such that the color luminance approximates the hill-shading brightness. Brewer and Marlow (1993) varied colors' lightness with aspect and chroma with slope. Kennelly and Kimerling's (2004) aspect color scheme was designed to complement hill-shading. Subtle variations in the luminosity of aspect colors highlight linear terrain features oriented parallel to the direction of illumination; these features are difficult to discern in traditional hill-shaded maps.

Such cartographic research falls under the umbrella of scientific or geographic visualization (Lo et al., 2002; Slocum et al., 2004), which includes methods of computation, cognition and graphic design (Buttenfield and Mackaness, 1991). Although geographic visualization of hill-shading with slope and aspect is well established, similar efforts with second derivative maps are not. Curvature map images provide detailed information about certain physical aspects of the terrain, but not in the context of overall shape. Maps often represent curvature in shades of gray, in a method similar to slope shaded maps (e.g. Wilson and Gallant, 2000; Li et al., 2004; El-Sheimy et al., 2005). Others use a diverging color scheme (Brewer, 2005), taking advantage of curvature values diverging away from flat terrain towards both concave upward and convex upward. Such a color scheme may vary from white in the center (flat) to dark blue (concave upward) and dark red (convex upward) at its ends (e.g. Wood, 1999).

This paper explores methods by which planimetric and profile curvature can be effectively imaged with hill-shading. The methods are based on illumination models, and have the potential to add useful information to the map. Such an image should match the viewer's cognitive model and help him/her understand the geographic context of patterns imaged. I begin by exploring the graphic limitations of first derivative maps, especially slope maps, on hill-shaded images from synthetic data. I then demonstrate how the same subtle variations in shape show more distinct patterns on second derivative maps. Finally, I show how these second derivative maps can be used to highlight physical features of real world data on hill-shaded maps.

2. Methods and models

To demonstrate that second derivative maps enhance patterns not obvious on hill-shaded maps or first derivative maps combined with hill-shading, I chose the simple geometric model of a cone. It is created from concentric contours with an interval of 50 m and with subsequent variations in radius of 100 m. The lowest contour is at a z-value of zero and the apex has a value of 1000 m.

From these contours, the cone everywhere would slope at 26.57°. To include a slope variation, all contours below 500 m were offset vertically by −1 m. The result is a band around the cone between elevations of 500 m and 449 m of slightly steeper slope (27.02°) than above or below, a difference in slope of 0.45°. The shape of the cone provides changes at all aspects. The contours are then converted into a triangulated irregular network (TIN), a series of adjacent triangular faces with each approximating the slope and aspect of the terrain in that area (Longley et al., 2005). The TIN in this study includes variations in aspect of faces from 0.5° to 5° of azimuth. The contours and edges of the triangular faces of the TIN are shown in Fig. 2.

The cone is then illuminated from a theoretical point light source to the northwest (N45°W) and at an angle 45° above the horizon. This hill-shaded representation shows very subtle variations in grayscale associated with the steeper slope, and these are only visible on the side of the cone opposite the illumination source (Fig. 3a). Quantifying the changes in hill-shading BV, shows why this change in slope is invisible or so difficult to see. On the illuminated side of the cone, these changes would account for a variation in BV of much less than one ($\Delta BV = 255(\cos 0° - \cos 0.45°) = 0.008$). Such a small change, therefore, could not be graphically represented. On the opposite side of the cone, these changes in BV would be a little more than two ($\Delta BV = 255 * (\cos 90° - \cos 89.55°) = 2.003$). Given the range of BV (0–255), a change of two units of BV would equate to a change in grayscale of less than 1%. Changes in BV with aspect vary greatly around the cone, which represents a ±180° change in azimuth. The smallest variations in aspect between adjacent triangular faces of the TIN (0.5°) would approximate those for slope quantified above.

A vertical illumination source applied to this same model provides a similar variation in shading within the band of steeper slope, with a change in BV compared to areas above or below the band of just less than two ($255(\cos 62.98° - \cos 63.43°) = 1.788$) (Fig. 3b). Fig. 3c shows hill and slope shading combined in a manner similar to the two

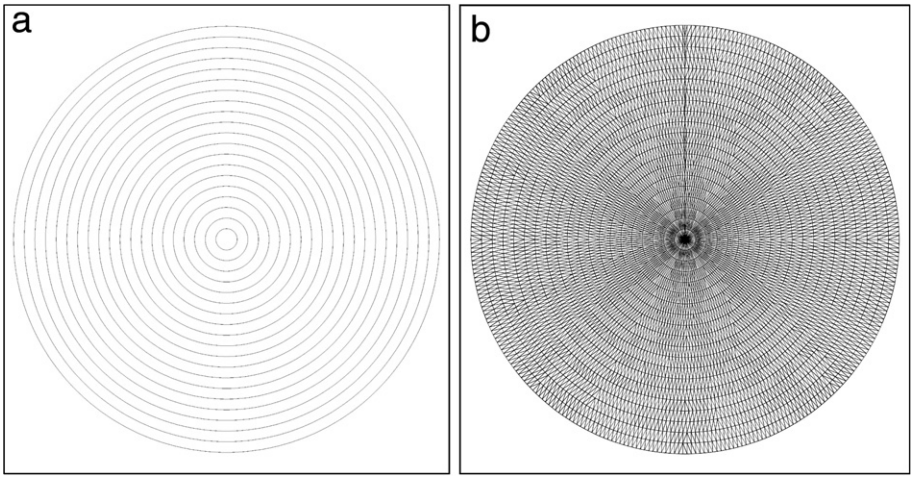

Fig. 2. Conic model to assess visibility of subtle changes in slope and aspect: a) unlabeled 50-m contours spaced at 100 m, with a small vertical offset of the lower half (see text) to show subtle variations in slope, and b) the triangulated irregular network (TIN) built from the contours (see text) to show subtle variations in aspect.

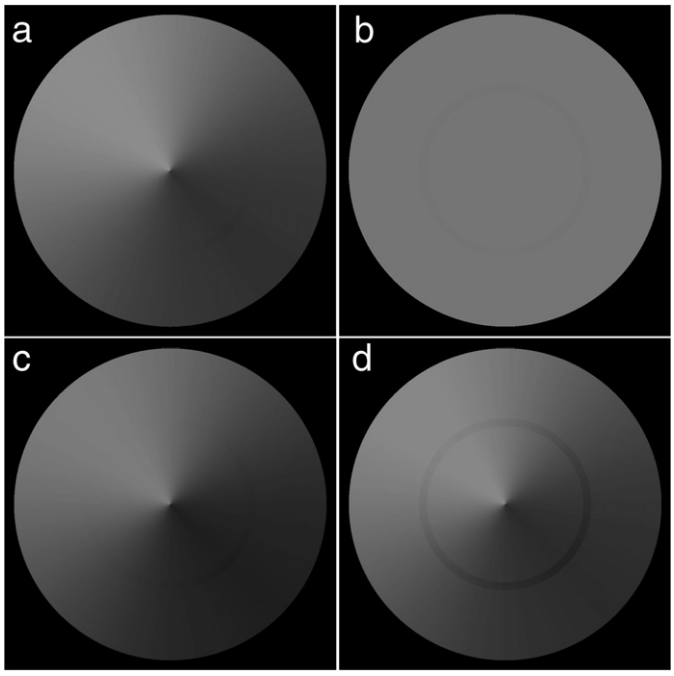

Fig. 3. Conic model hill-shaded with: a) oblique illumination, b) vertical illumination, c) combined oblique and vertical illumination, and d) combined oblique and enhanced-vertical illumination.

illumination models. The band of steeper slope is again more apparent on the side of the cone opposite the illumination source, but it can be traced closer to the illuminated side of the cone.

In this simple model, the binary nature of the slope shading provides additional potential for enhancing the more steeply sloping area. All surface elements have a BV of 116 (255*cos62.98°) or 114 (255*cos63.43°). As such, the mapmaker may choose to migrate the higher and lower BV values away from these extremely similar shades of gray towards the black and white end of the grayscale. This process is similar to "contrast stretching" or "level slicing" applied to enhancement of remote sensing imagery (Lillesand et al., 2004; Jensen, 2004; Aronoff, 2005).

Fig. 3d enhances the contrast of slope shading using the method, with the two shades of gray now varying by 10%. The darker band representing steeper slope is now apparent on the hill-shaded image. Although visually enhanced, this image may prove confusing to the viewer. He/she may predict a steeper slope to be similar to his/her cognitive model of what a cone illuminated in this manner "should" look like. Thus, adding slope shading to hill-shading may require a compromise between being true to the illumination model (Fig. 3c) or imaging a pattern with more contrast (Fig. 3d). Also, the contrast stretching technique would not work as effectively with real terrain data, as it would have a greater variation in the initial shades of gray that represent varying slopes.

Planimetric and profile curvature are next calculated for the cone. Fig. 4a images planimetric curvature, but it is difficult to see at this level of detail. The more detailed Fig. 4b reveals gray triangular faces with whiter edges, represented in a manner similar to slope shading. The shades of gray, however, convey different meanings. In slope shading, steeper slopes are darker. To show curvature, areas of curvature are lighter and areas of no curvature are an intermediate shade of gray.

The profile curvature map (Fig. 4c) highlights a fundamental difference between curvature and slope models. Whereas the anomalous band of steeper slope appears as a continuous band of darker gray in the slope map, only the edges of the band are highlighted by the profile curvature map. This second derivative map documents areas of change in slope as opposed to change in elevation. The same is true of the planimetric curvature map. All faces of the TIN are assigned the same shade of gray, as they include no changes in aspect. Only at the edges of the face does aspect change and planimetric curvature have a value not equal to zero.

The planimetric shading in Fig. 4b is also similar to diffuse illumination models. In all previous examples, the illumination source is a single, bright point in an otherwise dark sky whose direction is defined by an inclination and declination. Ideal diffuse illumination assumes equal brightness coming from all sectors of the sky. In this case, BV of surface elements would be a function of the distribution of light in the sky, and how much of the sky is visible from any given point (Kennelly and Stewart, 2006). Terrain models reveal that convex upward ridgelines and peaks are lighter than surrounding topography, because the maximum amount of the sky is visible. In terrain models, concave upward stream valleys are darkest close to the valley wall, and increase in lightness moving toward the center of the valley (Kennelly and Stewart, 2006). In an extreme case, an observer standing with his/her back against a vertical valley wall would necessarily have half of the sky blocked from view, but an observer at the center of the valley would have a larger percentage of the sky visible.

The profile shading in Fig. 4c is also similar to diffuse illumination. Along the top of the band, the slope is less-steep above and steeper below; along the bottom the opposite is true. The geometry results in more sky being visible from the top of the band and the resulting hill-shading being a lighter shade of gray. This is similar to the previous discussion, because terrain with less-steep slope above and steeper slope below would be convex upward. The profile curvature map is combined with hill-shading in Fig. 4d. The area of steeper slope is more apparent than in Fig. 3c, and is highlighted in a manner similar to a combination of diffuse and point source illumination.

3. Results

I used hill-shading with curvature enhancements to map a portion of the Mauna Kea volcano, Hawaii and the Grand Canyon, Arizona. Input data are part of the National Elevation Dataset obtained from the U.S. Geological Survey National Map Seamless Distribution System

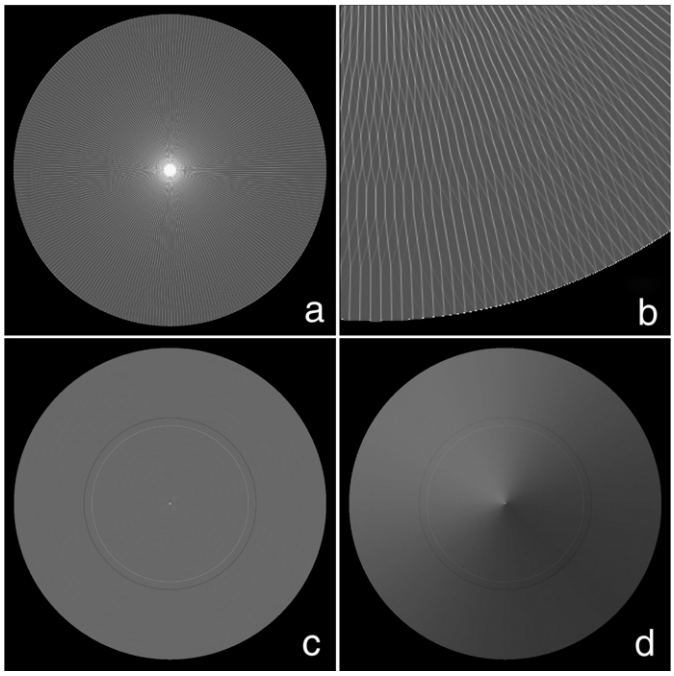

Fig. 4. Conic model shaded with a) planimetric curvature, b) planimetric curvature (close-up), c) profile curvature, and d) combined oblique illumination (Fig. 3a) and profile curvature (c).

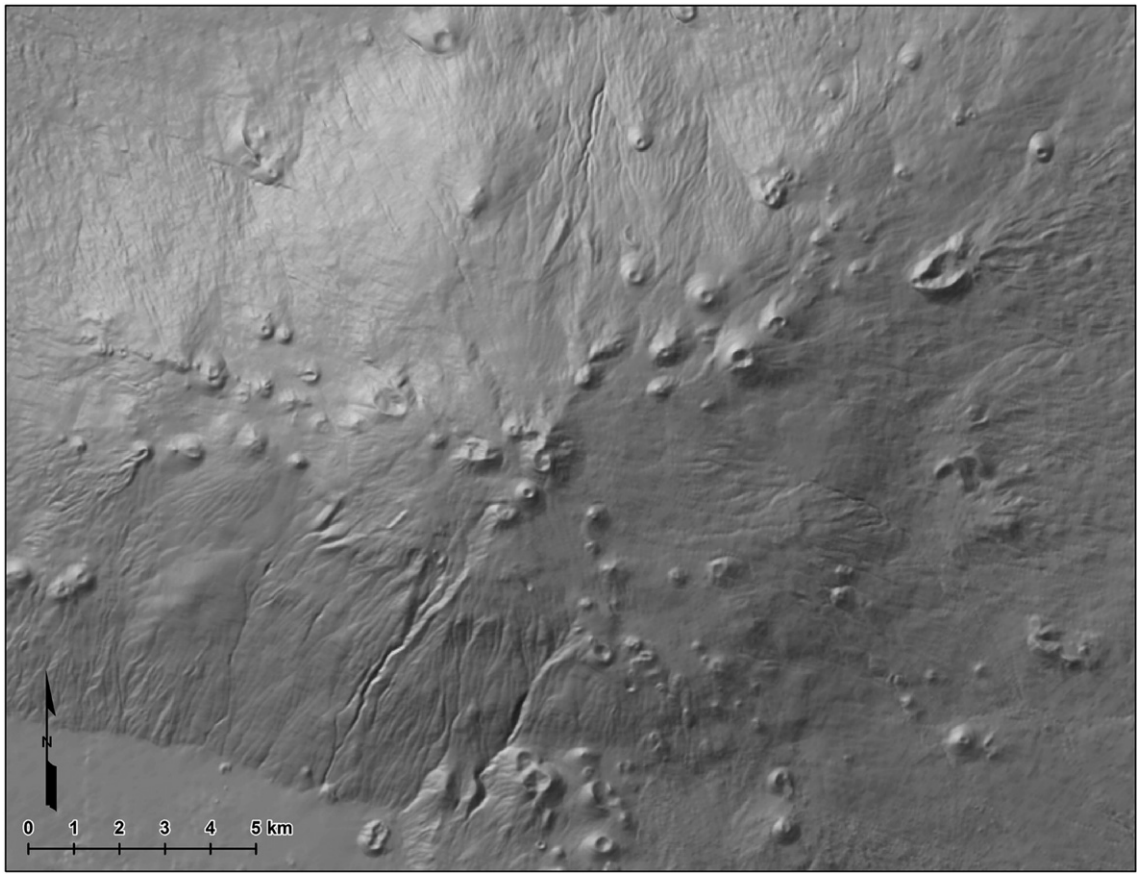

Fig. 5. Hill-shaded map of a portion of the Mauna Kea volcano, Hawaii.

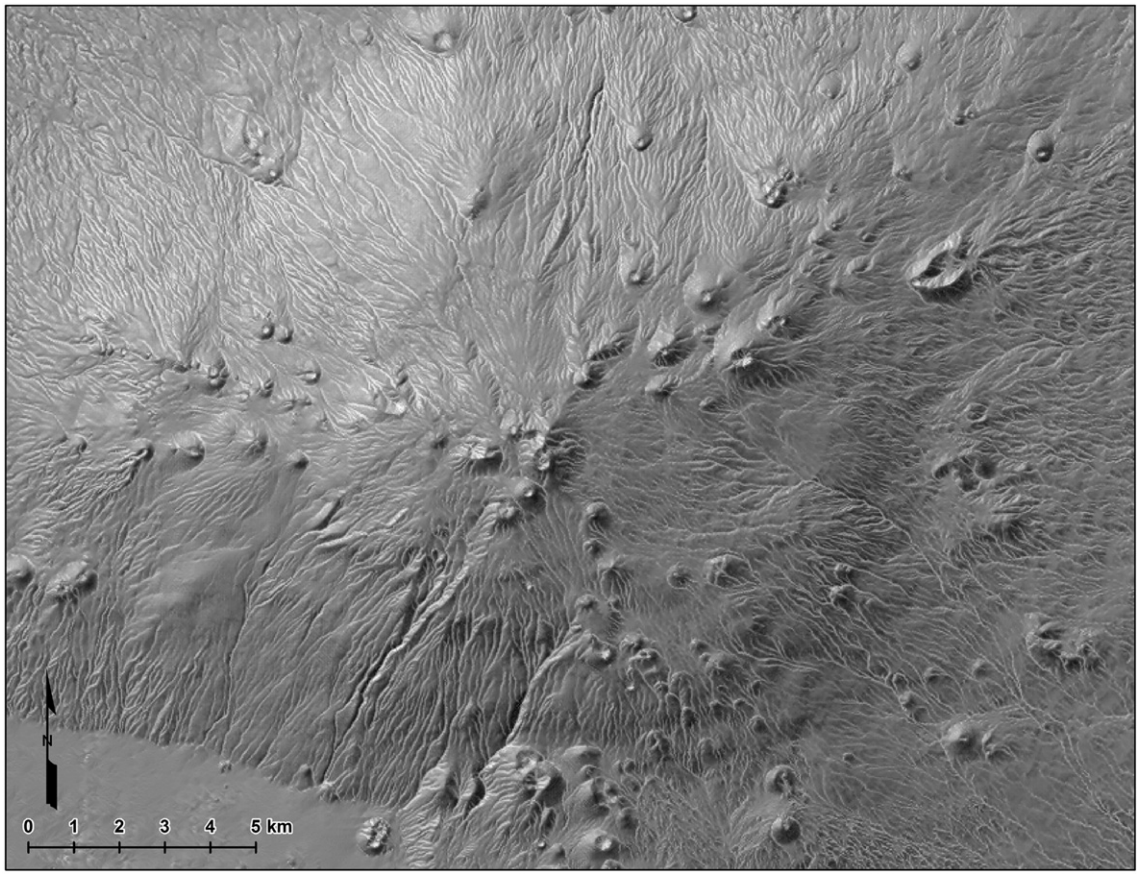

Fig. 6. Hill-shaded map of Mauna Kea enhanced by planimetric curvature.

website <http://seamless.usgs.gov>. The Hawaiian digital elevation model (DEM) has a resolution of one arc second, or approximately 29.8 m. The Grand Canyon DEM has a resolution of one-third arc second, or approximately 9.2 m. The Grand Canyon and the Mauna Kea volcano were chosen to illustrate geomorphologically interesting variations in slope and aspect, respectively. These DEMs also represent areas in which the ground is generally devoid of vegetative cover.

3.1. Planimetric curvature enhancements to hill-shading — Mauna Kea

Fig. 5 is a conventional hill-shaded map of the central portion of the Mauna Kea volcano on the Island of Hawaii. It is illuminated from a declination of 315° (N45°W) and an inclination of 45°, as are all subsequent hill-shaded maps. The map shows a broadly convex shield volcano and many cinder cones, some with craters. A weak radial drainage pattern is visible on the flanks of the volcano. These drainages are not necessarily streams, but channelized areas in which surface runoff may flow. Drainages oriented northeast and southwest, however, are more apparent than those oriented northwest and southeast. This lack of contrast for drainages oriented northwest or southeast is due to opposite sides of somewhat linear drainages having very different aspects, but having surface normal vectors that form a similar angle θ with the illumination vector. If the direction of illumination is changed to the northeast (N45°E), northwest and southeast drainages are better visible, but northeast and southwest ones are less visible.

Fig. 6 shows the same area in hill-shading enhanced by planimetric curvature. To match patterns of terrain under diffuse illumination, the shading legend is divergent; dark gray represents flat areas and white represents both concave and convex terrain. Drainages are now well delineated in all directions. This radial pattern should also help the map viewer to locate the volcano's peak at the pattern's hub. This drainage pattern is not nearly as apparent in Fig. 5.

Planimetric curvature is not the only topographic attribute with which drainages can be located. Hydrologic models are often combined with DEMs to define drainage networks (Olivera et al., 2002). This generally involves filling isolated lows associated with data sampling, determining the flow direction at each grid cell, and then summing flow accumulations throughout the entire grid. Fig. 7 shows a hill-shaded map containing a drainage network created in such a manner with the ArcHydro data model and ArcGIS software (Olivera et al., 2002). All grid cells with a flow accumulation of 50 grid cells or more are imaged as drainages in white.

Figs. 6 and 7 both show drainage networks, but with four important differences. First, drainages derived from hydrologic models are apt to follow linear trends, which are often a reflection of small systematic errors in the DEM. Such artifacts are apparent throughout Fig. 7. Second, the flow-accumulation model results in drainages that tend to be one grid cell wide. Hydrologic models accumulate data from the entire dataset, but are not designed to look at variations in elevation adjacent to the cells of greatest accumulation. These raster drainage networks can be converted into vector format to allow line thickness to change in a prescribed manner, but it would not be a trivial task to match line thickness to the actual width of the drainages. In Fig. 6, planimetric curvature provides an accurate rendering of the drainage width and is thus an improved visualization of the shape of drainages compared to Fig. 7.

Third, the hydrologic model used in this study assumes an impervious surface. Flow accumulates as a network based on how much area upland from a grid cell contributes surface water. The only logical downslope termini are closed depressions (those not recognized as data sampling artifacts and filled in the first step of the hydrologic modeling) or the ocean. This simple model does not take into consideration many factors that could terminate surficial flow such as local variations in infiltration. Southwest of Mauna Kea in

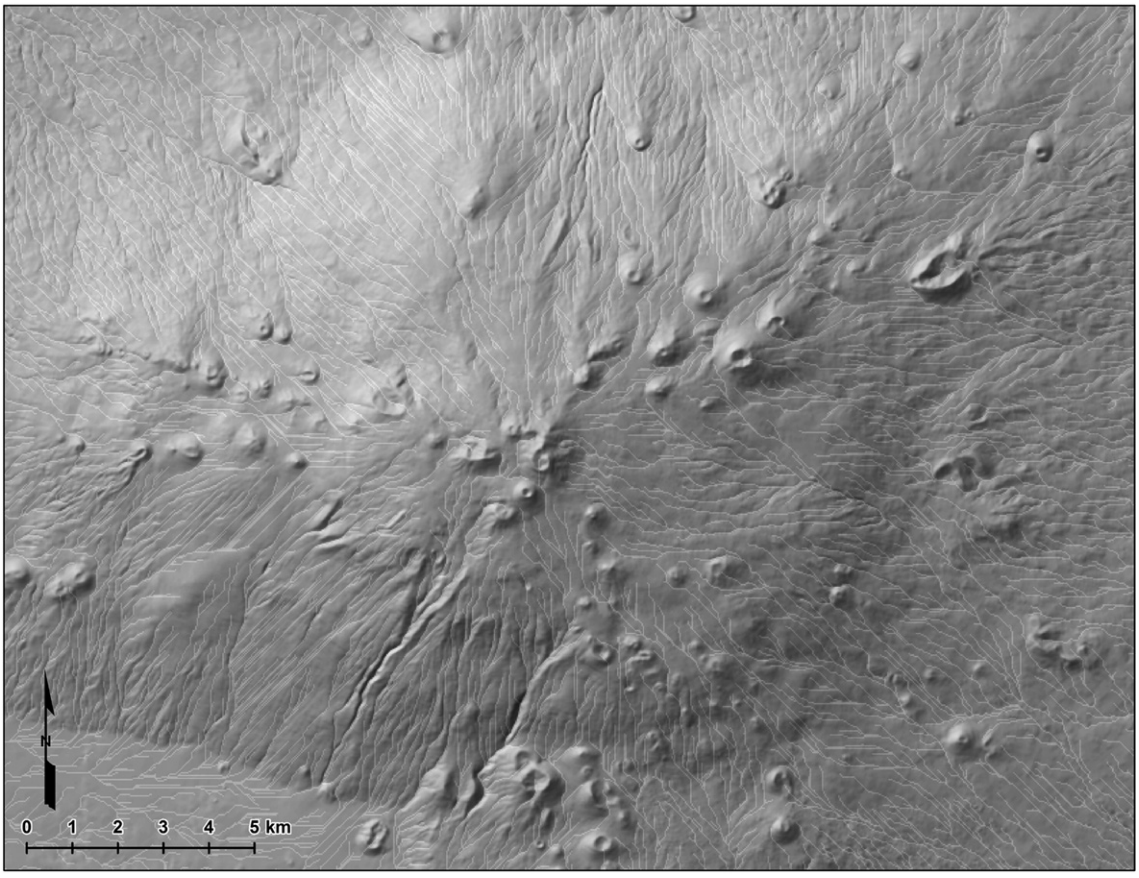

Fig. 7. Hill-shaded map of Mauna Kea with drainages derived from hydrological modeling shown in white.

Fig. 8. Hill-shaded map of a portion of the Grand Canyon, Arizona.

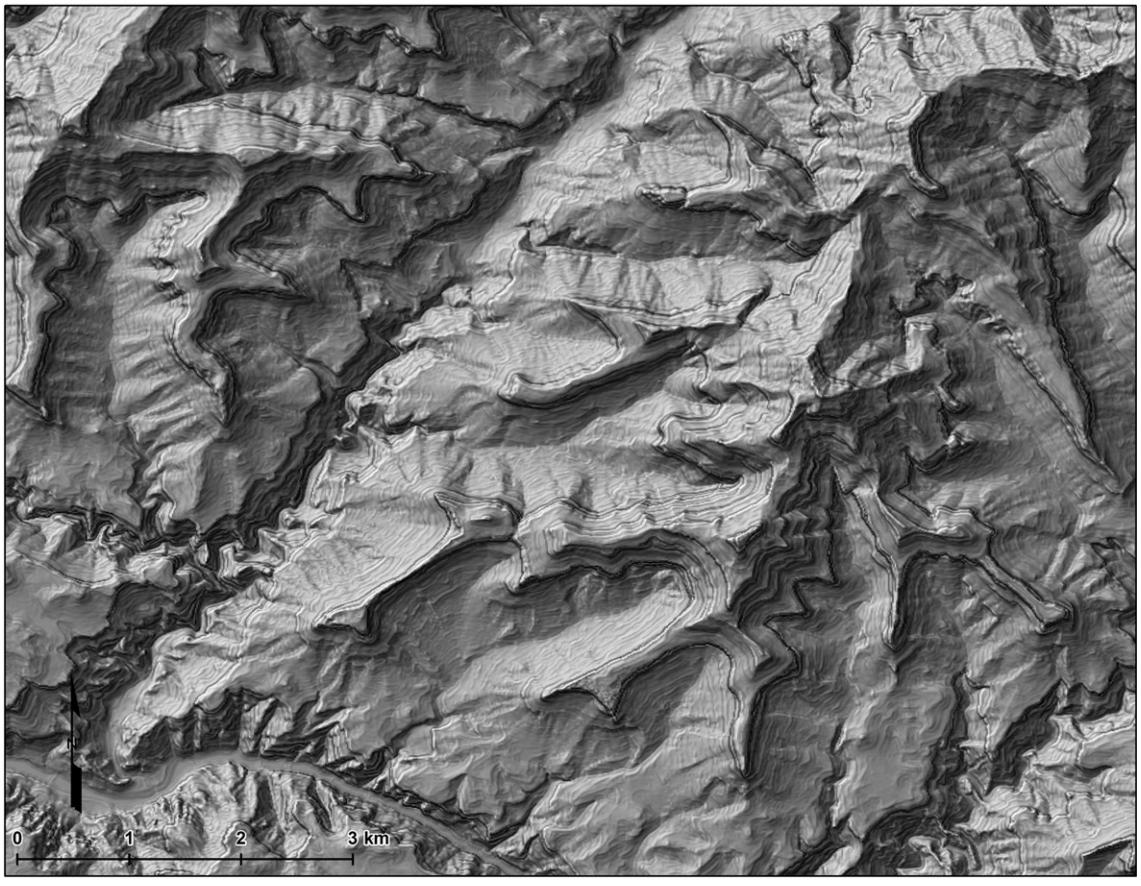

Fig. 9. Hill-shaded map of a portion of the Grand Canyon enhanced by profile curvature.

Fig. 7, for example, hydrologic modeling predicts that drainages will continue across the flat area at the volcano's base. Fig. 6 shows that no drainages are present here, as surface water arriving at the base of the volcano infiltrates the ground.

Fourth, the hydrologic data model is designed to model the accumulation of converging flow only (Fig. 7). Fig. 6 shows areas of converging and diverging flow. Imaging areas of divergent flow can be especially critical to geomorphologists in areas of deposition, such as alluvial fans, braided streams, distributary channels, or deltaic deposits.

3.2. Profile curvature enhancements to hill-shading — the Grand Canyon

Fig. 8 is a hill-shaded map of a portion of the Grand Canyon. It includes such features as Zoroaster Temple, Brahma Temple, Deva Temple, Sumner Butte, Hattan Butte, and portions of Bright Angel Creek. Several variations in slope are apparent from changes in shades of gray. The contrast is most pronounced on southeastern-facing canyon walls opposite the illumination source, as would be expected from the conic model.

Fig. 9 shows the same area displayed as hill-shading enhanced by profile curvature. The curvature information provides more detail to the map in a manner similar to combined diffuse and directional illumination. The method also adds texture to the image in two ways. First, image edges marking rapid changes of slope are delineated similarly across the map, from the weakly illuminated southeast side of landforms to the intensely illuminated northwest side. These variations appear to coincide closely with lithologic units, although the most detailed geologic mapping covering this area is at a scale of 1:100,000 (Billingsley, 2000). Second, subtle edges in the image roughly parallel the shape of contours within geologic units.

To examine the correspondence among these processing enhancements, geologic units, and terrain contours, I apply the same hill-shading methods to topography of the Cane quadrangle, Arizona. The associated DEM comprises grid cells approximately 9.5 m across and is located approximately 45 km northeast of Figs. 8 and 9. Detailed (1:24,000) geologic mapping (Billingsley and Wellmeyer, 2000) matches the detail of the 1:24,000 topographic mapping, which illustrates the relations among hill-shading, planimetric curvature, geologic units and changes in elevation. I focus on the portion of Cane Canyon shown in Fig. 10. The terrain is shown with hill-shading (a), and with hill-shading enhanced by planimetric curvature (b). These images are comparable in construction method with Figs. 8 and 9, respectively.

Some tonal variations in Fig. 10 reflect the geomorphology of the area, most notably the cliff that runs from northwest to southeast across the map. Others are artifacts of the DEM processing. This is especially evident in the terraced appearance of the northeast portion of this map. Comparing Fig. 10a and b, it is apparent that this method enhances geomorphologic features and systematic noise alike. It should be noted, however, that continuous tonal edges in Fig. 10b associated with the top of the cliff overprint the artifacts from contours.

Fig. 10c shows the relation between contours and curvature enhancement. A 40 foot contour interval was selected to match the interval of the original U.S. Geological Survey Cane quadrangle topographic sheet. Thicker index contours represent a change in elevation of 200 ft. The close correspondence between contours and tonal variations associated with profile curvature in the northeastern portion of the map is apparent. This systematic error may have been introduced when contours were interpreted from aerial photography, or when contours on the U.S. Geological Survey topographic sheets were sampled to create the DEM. Although not the primary focus of this method, profile curvature greatly enhances these artifacts and could be used for quality control purposes.

Fig. 10d shows the relations between some geologic units and the patterns of enhanced shading. All units in this map are lower Permian. The top and bottom of the Toroweap formation are defined by the upper and lower black bands. The Coconino Sandstone lies directly beneath the base of the Toroweap. The Coconino sandstone and other sandstone and limestone members of the Toroweap are important cliff formers in this area (Sorauf and Billingsley, 1991). The associated profile curvature enhances a distinctive pattern in Fig. 10b, both on the north and south canyon walls. On the north wall, the tonal edge is uninterrupted, even though elevation varies by over 400 ft.

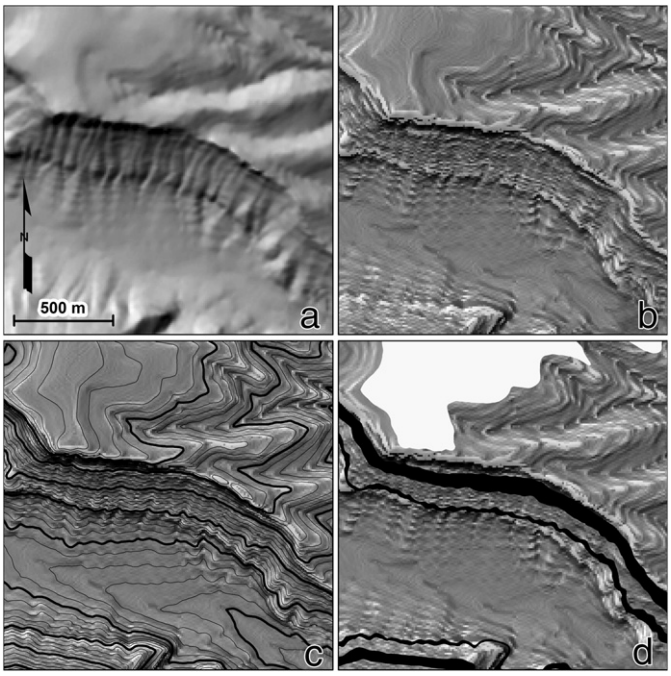

Fig. 10. Portion of the Cane quadrangle, Arizona, hill-shaded with oblique illumination and: a) unenhanced, b) enhanced by profile curvature, c) with added contours, and d) with geologic units overlain in black (top and bottom of the Toroweap Formation) and white (Harrisburg member of the Kaibab Formation).

The bottom of the canyon below the Coconino Formation comprises the silty sandstone and siltstone of the Hermit Formation. These slope formers (Sorauf and Billingsley, 1991) show curvature enhancements closely related to the spacing of contours. The portion of the map above the Toroweap Formation is the Kaibab Formation. The western plateau is capped by the Harrisburg member of the Kaibab, the location of which is overlain by a white polygon in Fig. 10d. The eastern portion is underlain by the Fossil Mountain member.

The Fossil Mountain member comprises fossiliferous, cherty limestones and sandy limestones, generally cliff formers (Sorauf and Billingsley, 1991). This is the area of the terraced pattern of tonal variations on the hill-shaded map enhanced with curvature. This is not to say, however, that all tonal variations derived from profile curvature that are parallel to contours are artifacts. In some instances, variations in geomorphology such as local lithologies showing more resistance to erosion create tonal enhancements in profile curvature.

Fig. 11 shows the area surrounding Sumner Butte in the Grand Canyon which demonstrates such local detail within a geologic unit. Fig. 11a is a map with conventional hill-shading, while Fig. 11b includes enhancements in profile curvature. There is an obvious tonal edge associated with the edge of the butte, which corresponds to the base of the Redwall Limestone. These tonal variations are enhanced in profile curvature, especially on the surface facing illumination. To the west of Sumner Butte is a localized cliff in the Mauv Limestone that is clearly visible on aerial photographs and satellite images. It is more apparent in the map with profile curvature enhancement, forming a halo to the west of the butte. Fig. 11c,d includes 40 and 200 ft contours and reveals that this tonal variation is related to subtle changes in contour spacing, which in turn reflect local variations in rates of

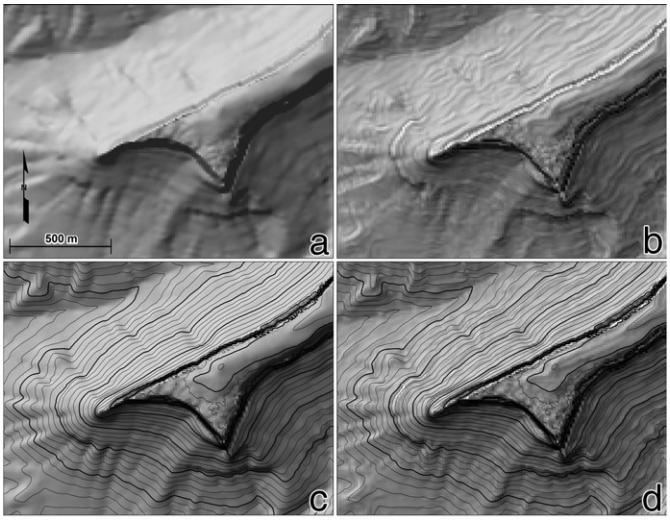

Fig. 11. Sumner Butte of the Grand Canyon with oblique hill-shading and a) unenhanced, b) enhanced by profile curvature, c) with added contours, and d) enhanced by profile curvature and with added contours.

erosion. Identifying such differences in curvature in the surrounding terrain could be important to geomorphologists looking for local variations in lithology, associated facies, or cementation.

In addition to enhancements related to differences in geomorphology, profile curvature does add other tonal variations to Fig. 11b that are faint artifacts of the DEM and its associated contours. These discontinuous tonal edges provide texture that helps to visually define the form of the terrain in a more subtle manner than including actual contours (compare with Fig. 11c).

In the above maps of Mauna Kea and the Grand Canyon, I chose to add grayscale variations associated with curvature to the hill-shading rather than varying color with curvature. I use this method because variations in grayscale can better reveal details while color elevation layer tinting shows variations over larger areas. Such a technique is commonly used with remote sensing data to merge multispectral data of lower resolution with panchromatic data of higher resolution (Lillesand et al., 2004; Jensen, 2004). Remote sensing analysts generally transform the color space of multispectral data from Red–Green–Blue (RGB) to Intensity–Hue–Saturation (IHS). A more detailed panchromatic band can then be substituted for the intensity (grayscale) band in the IHS image to provide a more detailed, color image.

Hill-shaded maps with layer tinting are often created with geographic information systems (GIS) software using the Hue–Saturation–Value (HSV) color model, where *V* is equal to the grayscale. *V* can then vary solely by hill-shading with curvature values, while layer tinting varies independently by both hue and saturation. Virtually any color of an artist's palette can then be assigned to mapped areas. As examples, Supplementary Material is provided for two maps of geologic units of Mauna Kea (Wolfe and Morris, 1996) and the Grand Canyon (Billingsley, 2000) layer tinted with color schemed from the U.S. Geological Survey.

4. Discussion

The images, their means of creation, and applications of the mapping techniques described here are similar to well established traditions in cartography and remote sensing. Adding curvature to hill-shaded images reprises the delineation of skeletal lines and the use of rock shading in the Swiss tradition. Highlighting local areas of rapid change in curvature is similar to edge-enhancement filtering in digital image processing. The usefulness of such images likely lies with the ability of the geomorphologist to make superior visual interpretations of them.

The cartographic technique advanced by Imhof (1965) employs skeletal lines to highlight the shape of the terrain and give organization to a relief map. Gross framework lines demarcate information-rich geomorphic features such as drainages, ridge lines, plateau edges, and crater rims. This framework can then be augmented by hill-shading to add detail. The map of Mauna Kea in

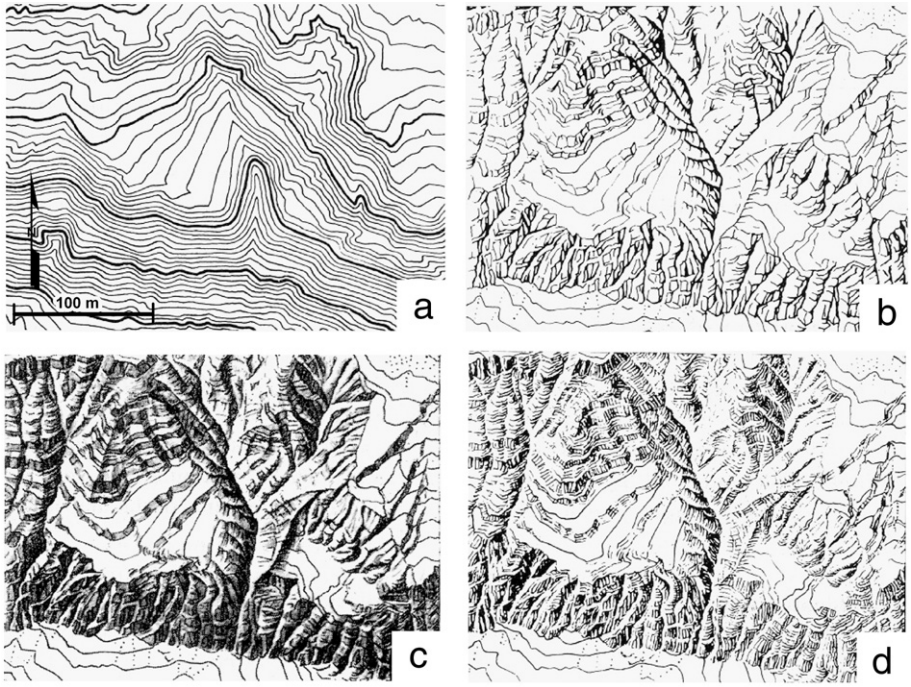

Fig. 12. The west wall of the Mürtschenstock, Switzerland illustrating Imhofs (1965) method of creating a) smooth 10-m contours, b) skeletal lines, c)rock shading, and d) rock hachures. (Used with permission [to be obtained] of Walter de Gruyter, Berlin and New York).

Fig. 6 is similar in its visual intent, the radial drainage pattern with curvature enhancements substituting for skeletal lines.

Cartographers distinguish between the gross framework and a detailed, internal framework of finer skeletal lines. These are associated with such geomorphic features as geologic units, bedding planes, and landslide margins (Imhof, 1965). This more refined framework sets the stage for rock shading, a very detailed method of terrain depiction designed to distinguish among rock strata. Fig. 12 is an example of maps by Imhof (1965) that transform information from contours (a) into gross and fine skeletal lines (b) and then renders the terrain with rock shading (c) and rock hachures (d), a form of shading that uses short strokes in the direction of aspect and of varying thickness to create tonal variation. Cartographers create these finer skeletal lines from contour spacing and detailed aerial photographs. The map of the Grand Canyon in Fig. 9 evidences the same style by highlighting curvature associated with a fine skeletal framework associated with variations in contour spacing between and within geologic units.

Curvature calculations are similar to edge-enhancement filters. Curvature calculations are applied to elevation data and use local variations within a moving window to determine concavity or convexity (See formulas in Chang, 2006). As this operation begins with elevation data, it can reveal details that, depending on the direction of hill-shading, may be invisible. Edge-enhancements are spatial filters applied to grayscale images of one band of the electromagnetic spectrum to calculate new values for each pixel centered in a moving window or convolution kernel (Lillesand et al., 2004; Jenson, 2004). The edge-enhanced image looks sharper because local contrasts are exaggerated. Because all curvature will be associated with some variation in slope and/or aspect, multiple hill-shaded maps illuminating a DEM from many different directions should reveal all of the changes that are apparent in hill-shaded maps with curvature. Previous studies illuminated terrain from multiple directions and combined results in one image, such as Mark's (1992) map of the island of Hawaii.

In remote sensing, edge-enhanced images are often combined with the original image to show high-and low-spatial frequency information simultaneously (Jensen, 2004). In a similar manner, tonal variations associated with curvature and hill-shading combine second and first derivatives of elevation data. Although it may be possible to use these maps for automated image extraction, the most obvious application is improving the geomorphologist's ability to visually interpret fine surficial features within the broader terrain.

5. Conclusions

Subtle details of the terrain are important to both geomorphologists and cartographers. Many quantitative techniques for defining topographic attributes and displaying images are available to both disciplines. This paper shows that changes in slope gradient of as little as 0.5° can be recognized in maps of profile curvature. These highlighted tonal edges do not disappear on the illuminated side of terrain if combined with traditional hill-shading methods. Combining hill-shading and curvature with directional and diffuse illumination as shades of gray in the accepted manner yields a rendering consistent with cognitive models of the map user.

Enhancing a hill-shading of the Mauna Kea volcano, with planimetric curvature highlights the radial drainage pattern. These drainages are clearly visible on all sides of the volcano, including that most brightly illuminated by the directional lighting associated with hill-shading. Although other means such as hydrologic modeling could image these drainages, such methods do not easily account for all local variations, especially divergent flow and infiltration. Enhancing a portion of the Grand Canyon with profile curvature highlights tonal edges between and within geologic units associated with changes in slope. Enhancements make the continuity of prominent geologic contacts more visually continuous on strongly illuminated faces. Also, subtle variations in slope or contour spacing within units result in discontinuous edges that add detail and texture to the map similar to that of the topography.

The methods developed in this study are designed to synthesize terrain variables in a single image and follow traditional practice in cartography and remote sensing. The method resembles that of defining skeletal lines, the basis for creating rock-shaded maps, in the Swiss cartographic tradition. Also, slope curvature creates effects that mimic a remote sensing edge-detection filter. Finally, the resulting images allow geomorphologists to interpret the landscape by combining their knowledge with the best geographic visualization.

Acknowledgements

I thank Dr. Takashi Oguchi of the University of Tokyo for editorial guidance and comments; Dr. Richard Pike of the U.S. Geological Survey for helpful feedback; George Billingsley and Susan Priest of the U.S. Geological Survey for providing the color palette for the map of the Grand Canyon; and Susan Vuke of the Montana Bureau of Mines and Geology for identifying prospective areas for detailed geologic and topographic comparison.

Appendix A. Supplementary data

Supplementary data associated with this article can be found, in the online version, at doi:10.1016/j.geomorph.2008.05.046.

References

Allan, S., 1992. Design and production notes for the Raven Map editions of the U.S. 1/3.5 million digital map. Annals of the Association of American Geographers 82, 303–304.
Aronoff, A., 2005. Remote Sensing for GIS Managers. ESRI Press, Redlands. 524 pp.
Billingsley, G.H., 2000. Geologic map of the Grand Canyon 30'×60' Quadrangle, Coconino and Mohave Counties, Northwestern Arizona. U.S. Geological Survey Geologic Investigations Series I-2688 Version 1.0.
Billingsley, G.H., Wellmeyer, J.L., 2000. Geologic map of the Cane Quadrangle, Coconino County, Northern Arizona. US Geological Survey, Miscellaneous Field Studies MF-2366 (pamphlet accompanies map).
Brewer, C.A., 2005. Designing Better Maps: A Guide for GIS Users. ESRI Press, Redlands, p. 203 pp.
Brewer, C.A., Marlow, K.A., 1993. Computer representation of aspect and slope simultaneously. Proceedings, Eleventh International Symposium on Computer-Assisted Cartography (Auto-Carto-11), Minneapolis, Minnesota, pp. 328–337.
Buttenfield, B.P., Mackaness, W.A., 1991. Visualization. In: Maguire, D.J., Goodchild, M.F., Rhind, D.W. (Eds.), Geographic Information Systems. Principles, vol. 1. Longman Scientific and Technical, Harlow, pp. 427–443.
Chang, K., 2006. Introduction to Geographic Information Systems, 4th ed. McGraw-Hill, New York. 450 pp.
El-Sheimy, N., Valeo, C., Habib, A., 2005. Digital Terrain Modeling: Acquisition, Manipulation and Applications. Artech House Publishers, Boston. 270 pp.
Evans, I., 1972. General geomorphometry, derivatives of altitude and descriptive statistics. In: Chorley, R.J. (Ed.), Spatial Analysis in Geomorphology. Harper and Row, New York, pp. 17–90.
Horn, B.K.P., 1981. Hill shading and the reflectance map. Proceedings of the Institute of Electrical and Electronics Engineers, vol. 69 (1), pp. 14–47.
Imhof, E., 1965. Kartographische Geländedarstellung. Walter de Gruyter, Berlin. 425 pp.; English translation published as Steward, H.J., ed., 1982, Eduard Imhof, Cartographic Relief Representation. Walter de Gruyter, New York, 389 pp.
Jensen, J.R., 2004. Introductory Digital Image Processing, (3rd Ed.). Prentice Hall, Upper Saddle River. 544 pp.
Kennelly, P., 2002. GIS applications to historical cartographic methods to improve the understanding and visualization of contours. Journal of Geoscience Education 50 (4), 428–436.
Kennelly, P., Kimerling, A.J., 2001. Modifications of Tanaka's illuminated contour method. Cartography and Geographic Information Science 28 (2), 111–123.
Kennelly, P., Kimerling, A.J., 2004. Hillshading of terrain using layer tints with aspect-variant luminosity. Cartography and Geographic Information Science 31 (2), 67–77.
Kennelly, P., Stewart, J., 2006. A uniform sky model to enhance shading of terrain and urban elevation models. Cartography and Geographic Information Science 33 (1), 21–36.
Li, Z., Zhu, Q., Gold, C., 2004. Digital Terrain Modeling: Principles and Methodology. CRC Press, Boca Raton. 323 pp.
Lillesand, T.M., Kiefer, R.W., Chipman, J.W., 2004. Remote Sensing and Image Interpretation. John Wiley and Sons, Inc., New York. 763 pp.
Lo, C.P., Young, A.K.W., 2002. Concepts and Techniques of Geographic Information Systems. Prentice-Hall, Upper Saddle River. 492 pp.

Longley, P.A., Goodchild, M.F., Maguire, D.J., Rhind, D.W., 2005. Geographic Information Systems and Science, (2nd ed.). Wiley, New York. 536 pp.
Mark, R., 1992. A multidirectional, oblique-weighted, shaded-relief image of the Island of Hawaii. U.S. Geological Survey Open-File Report 92-422. 3 pp., http://wrgis.wr.usgs.gov/open-file/of92-422/of92-422.pdf.
McCullagh, M.J., 1998. Quality, use and visualisation in terrain modeling. In: Lane, S.N., Richards, K.S., Chandler, J.H. (Eds.), Landform Monitoring, Modeling and Analysis. John Wiley & Sons, Chichester, pp. 95–117.
Moellering, H., Kimerling, A.J., 1990. A new digital slope-aspect display process. Cartography and Geographic Information Systems 17, 151–159.
Oguchi, T., Aoki, T., Matsuta, N., 2003. Identification of an active fault in the Japanese Alps from DEM-based hill shading. Computers and Geosciences 29, 885–891.
Olivera, F., Furnans, J., Maidment, D., Djokic, D., Ye, Z., 2002. Drainage systems. In: Maidment, D.R. (Ed.), Arc Hydro: GIS for Water Resources. ESRI Press, Redlands, pp. 55–86.
Patterson, T., 2004. Creating Swiss-style Shaded Relief in Photoshop. [http://www.shadedrelief.com/shading/Swiss.html.].
Patterson, T., Hermann, M., 2004. Creating Value-enhanced Shaded Relief in Photoshop. [http://www.shadedrelief.com/value/value.html.].
Peucker, T.K., Tichenor, V., Rase, W.D., 1975. The computer version of three relief representations. In: Davis, J.C., McCullagh, M. (Eds.), Display and Analysis of Spatial Data. John Wiley and Sons, New York, pp. 187–197.
Robinson, A.H., Morrison, J.L., Muehrcke, P.C., Kimerling, A.J., Guptill, S.C., 1995. Elements of Cartography, 6th ed. John Wiley and Sons, New York. 688 pp.
Slocum, T., McMaster, R., Kessler, F., Howard, H., 2004. Thematic Cartography and Geographic Visualization, 2nd ed. Pearson Prentice-Hall, Inc., Upper Saddle River. 528 pp.
Smith, M.J., Clark, C.D., 2005. Methods for the visualization of digital elevation models for landform mapping. Earth Surface Processes and Landforms 30, 885–900.
Sorauf, J.E., Billingsley, G.H., 1991. Members of the Toroweap and Kaibab Formations, Lower Permian, northern Arizona and southwestern Utah. The Mountain Geologist 28 (1), 9–24.
Tanaka, K., 1932. The orthographic relief method of representing hill features on a topographic map. Geographical Journal 79, 213–219.
Tanaka, K., 1950. The relief contour method of representing topography on maps. Geographical Review 40, 444–456.
Thelin, P., Pike, R., 1991. Landforms of the conterminous United States—a digital shaded-relief portrayal. Technical Report I-2206, U.S. Geological Survey Miscellaneous Investigations Series Map (map and accompanying text). 16 pp.
Van Den Eeckhaut, M., Poesen, J., Verstraeten, G., Vanacker, V., Moeyersons, J., Nyssen, J., van Beek, L.P.H., 2005. The effectiveness of hillshade maps and expert knowledge in mapping old deep-seated landslides. Geomorphology 67, 351–363.
Wilson, J.P., Gallant, J.C., 2000. Digital terrain analysis. In: Wilson, J.P., Gallant, J.C. (Eds.), Terrain Analysis: Principles and Applications. John Wiley & Sons, New York. 1–27.
Wolfe, E.W., Morris, J., 1996. Geologic map of the Island of Hawaii. U.S. Geological Survey Miscellaneous Investigations Series Map I-2524-A (3 sheets, descriptive pamphlet).
Wood, J.D., 1999. Visualisation of scale dependencies in surface models. International Cartographic Association Annual Conference, Session 37-B, Ottawa, Canada, presentation. http://www.soi.city.ac.uk/~jwo/ica99/.
Yoeli, P., 1983. Shadowed contours with computer and plotter. The American Cartographer 10 (2), 101–110.